INTERACTIONS BETWEEN 7.5-GeV π-MESONS AND NUCLEONS AND THEIR ANALYSIS ON BASIS OF POLE DIAGRAMS

A. Kh. VINITSKIĬ, I. G. GOLYAK, V. I. RUS'KIN, and Zh. S. TAKIBAEV

Nuclear Physics Institute, Academy of Sciences, Kazakh S.S.R.

Submitted to JETP editor July 28, 1962

J. Exptl. Theoret. Phys. (U.S.S.R.) **44**, 424-430 (February, 1963)

Results of a study of 200 inelastic pion-nucleon interaction events are discussed. The angular and momentum characteristics of the secondary particles are presented and are found to possess a number of special features. Thus, the pion angular distributions are asymmetric and are peaked in the forward direction; the nucleon distribution is peaked in the backward direction. In stars with a few prongs the pion and nucleon momentum curves have two peaks. Angular correlations between two pions are considered. The experimental data are analyzed from the standpoint of pole diagrams describing interactions involving one- two- and three-pion systems. The diagrams considered can explain about a third of the inelastic pion-nucleon interaction events of low multiplicity.

EXPERIMENTAL RESULTS

We carried out a study of πN interactions recorded in emulsion exposed at the proton synchrotron of the Joint Institute of Nuclear Research (Dubna). We scanned 900 m of primary track and found 2100 interactions with emulsion nuclei. The cases of πN interactions were selected by criteria described in the literature.[1] From all the interactions we selected 200 cases of inelastic πN interaction.[1)] The prong distribution for these events is given in Table I. Also shown in this table are the distributions found in other experiments[2,3] and calculated from the statistical theory with allowance for the isobaric states.[4] It is seen that the percentage of cases with different multiplicity agrees only approximately with the experimental data found in other experiments and with the distribution calculated from the statistical theory. A difference occurs in the case of three- and seven-prong stars.

To calculate the angular and energy characteristics of the secondary particles we identified all particles whose dip angle φ relative to the emulsion plane was $\leq 8°$. Here we used a method developed by us earlier.[5] We identified a total of 323 particles, of which 259 proved to be pions, 19 were K mesons, and 45 were protons. Particles with momentum between 1.5 and 2.5 GeV, which are difficult to identify, were classified as pions.[2] However, the number of such particles was small and they did not affect the final results. To take into account particles with large dip angles we introduced geometrical corrections.[6]

Figures 1a, b, c display the pion c.m.s. angular distributions for stars of various multiplicity. It is seen that the pion angular distributions are asymmetric with a peak in the forward direction, but the degree of asymmetry drops with the multiplicity, in agreement with the results obtained by other authors.[2,3]

The proton c.m.s. angular distribution is shown in Fig. 2. All protons are emitted preferentially in the backward direction, i.e., they preserve their initial direction. It should be noted, however, that, in contrast to pions, the degree of asymmetry is independent of the multiplicity.

Figures 3 and 4 show the pion and proton momentum distributions for different multiplicities. In the momentum distribution the protons have two maxima: in the region 0.4—0.6 and 1.4—1.6 GeV/c. For pions, a tendency to the formation of maxima is also observed, especially for small multiplicities, in the intervals 0.2—0.4 and 0.6—0.8 GeV/c.

Table II lists the values of the mean total and transverse momenta of $\pi^{\pm}$ mesons as a function of the multiplicity. Also listed there are the mean pion momenta taken from the data in the literature. It is seen that for pions $p_{\perp}$ does not depend on the multiplicity.

During the identification of particles we ob-

[1)]Since inelastic interactions leading to one-prong stars are very difficult to distinguish from elastic π^-N scattering, cases with $n_s = 1$ were not included in our statistics.

Table I

		Multiplicity n_s						
		2	4	6	8	3	5	7
Present work	N_{int}	48	45	11	1	56	29	10
	%	45.7±6.0	42.8±6.4	10.5±3.2	0.9±0.9	59.0±7.9	30.5±5.7	10.5±3.3
Data of [3]	N_{int}	119	115	20	1	53	21	3
	%	46.7±4.3	45.2±4.2	7.8±1.7	0.4±0.4	68.8±9.5	27.3±5.9	3.9±2.3
Data of [2]*	N_{int}	142	122	14	2	143	36	7
	%	50.7±4.3	43.6±3.8	5.0±1.3	0.7±0.5	77.0±6.4	19.3±3.2	3.8±1.4
Statistical theory [4], %		48	46	6,3	0.1	73.6	23.8	2.5

*One-prong stars are excluded (N_{int} is the number of interactions).

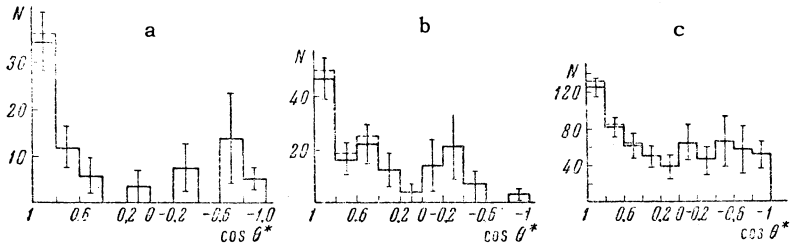

FIG. 1. Pion c.m.s. angular distribution: a – two-prong stars, b – three-prong stars, c – all stars (the dashed line represents the distribution with allowance for pions falling in the region in which identification is difficult).

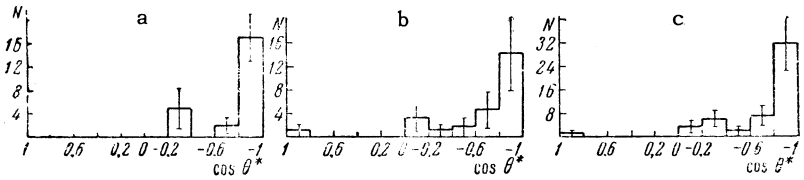

FIG. 2. Proton c.m.s. angular distribution: a – 2-, 4-, 6-, and 8-prong stars; b – stars with n_s equal to 3, 5, and 7; c – all stars.

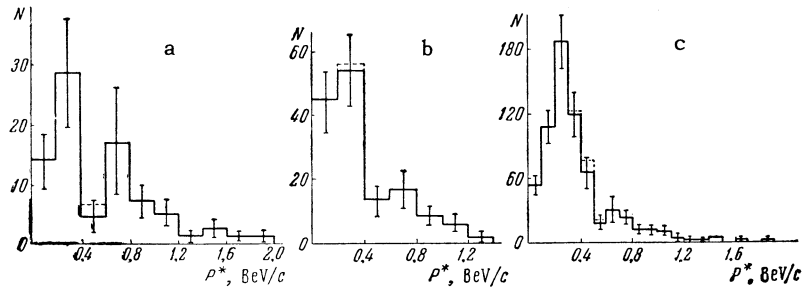

FIG. 3. Pion c.m.s. momentum distribution: a – two-prong stars; b – three-prong stars; c – all stars (the dashed line includes pions from the region where the identification is difficult).

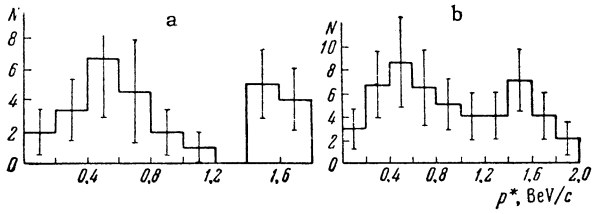

FIG. 4. Proton c.m.s. momentum distribution: a – two- and three-prong stars; b – all stars.

served in 16 πN interactions 19 particles which did not lie on either the pion or proton curves and which were most likely K mesons.[8]

We studied the angular correlations between pairs of particles in two- and three-prong stars.

We determined the space angle $\theta_{\pi\pi}$ between the two pions in the c.m.s., which could only be done in cases in which both pions were identified (Fig. 5, dashed line). However, since we only attempted to identify particles with dip angles $\varphi \leq 8°$, there is no guarantee against a possible bias. In order to take into account the unidentified particles in this distribution, it was assumed that they were pions and that the shape of the $p_\perp$ distribution for them was the same as for the identified particles (Fig. 5, solid line). These assumptions are based on the fact that the number of high-energy protons (ionization $g/g_0 \leq 1.4$) is small and that allowance for the shape of the transverse momenta distribution[9] leads to a small error in the angular distribution.

Table II

n_s	$\bar{p}^*$, BeV/c			$\bar{p}_\perp$, BeV/c
	Present experiment	Dubna [2]	Berlin [7]	Present experiment
2	0.60±0.07	0.62±0.06	0.60±0.05	0.23±0.05
3	0.39±0.05	0.44±0.04	0.55±0.04	0.24±0.04
4	0.39±0.07	0.52±0.05		0.25±0.04
5,6,7,8	0.31±0.07	0.46±0.06	0.35±0.03	0.25±0.05
All stars	0.38±0.03	0.53±0.03	0.50±0.03	0.25±0.03

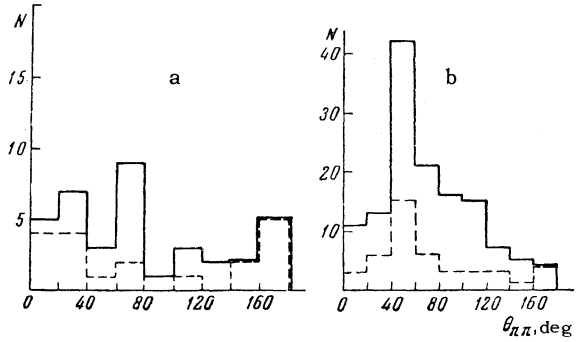

FIG. 5. Angular correlations: a – two-prong stars; b – three-prong stars (the solid line represents all particles, the dashed line represents the identified particles).

2. ANALYSIS OF THE EXPERIMENTAL DATA

The experimental data were analyzed from the viewpoint of the peripheral interactions.[10] We considered the pole diagrams represented in Fig. 6. Since there is no reliable information (theoretical or experimental) about the vertices of these diagrams, the basic attention was paid to the calculation of the kinematic characteristics.

Diagrams a and b were calculated under two assumptions as regards the shape of the $\sigma_{\pi\pi}$ cross sections: 1) $\sigma_{\pi\pi}(\omega^2)$ = const and 2) $\sigma_{\pi\pi}$ is described by the Breit-Wigner formula for $\pi\pi$ scattering in the T = 1, J = 1 state (T is the isospin and J is the ordinary spin).[11] In the calculation

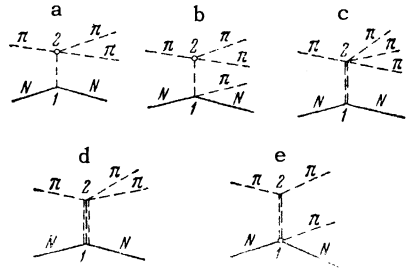

FIG. 6. Feynman diagrams for interactions proceeding through the exchange of one-, two-, and three-pion systems.

of diagram b we computed $\sigma_{\pi N}(\mathfrak{M})$ in both cases from the Breit-Wigner formula for πN scattering in the T = J = 3/2 state.

The existence of a resonance in the ππ interaction with T = J = 1 and resonance energy 750 MeV, and a three-pion resonance with T = 0, J = 1 and the same resonance energy has recently been established. The lifetimes of these resonant systems are $\sim 10^{-22}$–10^{-23} sec, which allows them to be considered within the framework of strong interactions as "stable" particles.

Diagrams c, d, and e represent the πN interaction proceeding through the exchange of these particles. The cross section for such processes in the c.m.s. can be written in the form of the following equations.

For diagrams c and d:

$$\sigma_{\pi N} = \frac{NE_0}{|\bar{P}_0|^2 W^2} \iint \frac{E_1 \omega \left[(\omega^2 + M^2 - \mu^2)^2 / 4\omega^2 - M^2\right]^{1/2}}{(\Delta^2 + M^2)^2} \times \left[2 - \frac{m^2}{E_0 E_1}\right] \sigma_2'(\omega^2)\, d\Delta^2\, d\omega^2,$$

where W, E_0, E_1 are the total energy, and the c.m.s. energies of the incident and scattered nucleons; $\bar{P}_0$ and $\bar{P}_1$ are the space momenta of these nucleons; m, μ, and M are the rest masses of the nucleon, pion, and the exchanged resonant system (in these calculations we took M = 550 MeV; allowance for the resonant systems with M = 750 MeV leads to approximately the same results); ω is the total energy of vertex 2 in its rest system; Δ^2 is the square of the 4-momentum of the intermediate particle.

For diagram e:

$$\sigma_{\pi N} = \frac{N}{|\bar{P}_0|\, W^2} \iint \frac{|\bar{P}_1|\left[(\mathfrak{M}^2 + M^2 - m^2)^2 - 4\mathfrak{M}^2 M^2\right]^{1/2}}{(\Delta^2 + M^2)^2} \times \left[M^4 - 4\mu^2 M^2\right]^{1/2} \sigma_1'(\omega^2)\, \sigma_2'(\mathfrak{M}^2)\, d\mathfrak{M}^2\, d\cos\theta.$$

In the calculations we assumed that $\sigma_1'(\omega^2)$ = const and $\sigma_{\pi N}(\mathfrak{M}^2)$ = const. In both cases the

integration was carried out without a cutoff in the virtuality.

The analysis showed that diagrams b—e give the main contribution to the region of the high-energy peak in the proton momentum distribution at 1.6—1.4 GeV (see Fig. 4a). The most probable value of the proton momenta P = 1.75 GeV/c, calculated from diagram a, does not coincide with the maximum in the experimentally found spectrum. It should be noted, however, that part of the protons can be lost in the experiment, owing to the selection criteria (in the l.s. these particles give short black tracks). From Fig. 4a it is seen that a maximum occurs in the energy region between 0.4 and 0.6 GeV. This maximum can be connected with the pole diagram of type d, where the internal line is a three-pion system with J = 0 and mass ~ 550 MeV. We denoted this diagram by the letter f. It differs from diagram d only by the presence of a pseudoscalar coupling instead of vector coupling at vertex 1.

The pions in diagrams a, c, d, and f[sic] give a contribution to the region of the high-energy peak at 0.6—0.8 GeV/c (Figs. 3a and 3b). In diagrams b and e, apart from high-energy pions (of momentum 0.7 GeV/c) from the pion vertex decay, there are pions of momentum ~ 0.3 GeV/c from the decay of an excited nucleon. It should be noted that the experimentally found value of the low-energy peak is much larger than that which is expected from the foregoing diagrams. In diagram e, a high-energy pion of momentum 1.6 GeV/c is produced at vertex 2; it cannot be distinguished from pions from diffraction scattering.

The nucleon angular distribution for all the diagrams is strongly asymmetric with a peak for backward emission, which agrees with experiment (Fig. 1). However, for each of the diagrams c—e there is a 20% probability that the nucleon is emitted in the forward hemisphere. Since the number of such protons observed experimentally is 5—6% (Fig. 2), the total cross section for these diagrams is probably small. The pion angular distribution is also asymmetric, but it has a peak in the forward direction, and the degree of asymmetry is less than the case of nucleons, which also does not contradict the experimental results (Fig. 1)

We also calculated the angular correlations of pions. From the figure it is seen that in two-prong stars two peaks are observed experimentally for the identified particles: between 0° and 40° and between 140° and 180°. If it is assumed that $P_\perp$ = const (see Sec. 1) then an additional peak appears in the region between 60° and 80°. In three-prong stars a sharp peak is observed experimentally in the angular region 40—60° (Fig. 5b). Under the condition that $P_\perp$ = const for the unidentified particles, the shape of this distribution does not change.

Diagrams a and d contribute to the angular region ~ 30°; diagram b gives two peaks: at 20° and 160°; diagram f gives a peak in the region of 60°; in diagram c, the method[12] used for calculation of the angular correlations is inapplicable.

3. CONCLUSIONS

The multiplicity distribution of the stars agrees within the limits of error with the conclusions of statistical theory. The pion c.m.s. angular distribution is asymmetric with a peak in the forward direction, but the degree of asymmetry drops with increasing multiplicity. The proton angular distribution is also asymmetric with a peak in the backward direction, but the degree of asymmetry is independent of the multiplicity. The momentum distributions of protons and pions have two maxima, which are most distinctly manifested in stars with a small number of prongs.

Analysis of the momentum and angular characteristics as well as the angular correlations in two- and three-prong stars shows that they have a number of characteristic features which can be explained from the standpoint of the pole diagrams considered by us. The fraction of cases which can be ascribed to these diagrams is at least 30%. The kinematic characteristics of all the pole diagrams, with the exception of diagram f, proved to be close to one another, and therefore we cannot make any quantitative estimate of the contribution from each of them. We can, however, draw qualitative conclusions. Diagrams b and f correspond best to the experimental results. This would favor the important role of processes proceeding through the production of a $\pi\pi$ resonant system and a nucleon isobar, and possibly indicate the important role of the exchange of a resonant 3π system with J = 0.

In conclusion the authors express their gratitude to the laboratory staff who took part in the measurements and calculations.

[1] W. D. Walker and J. Crussard, Phys. Rev. **98**, 1416 (1955); N. G. Birger and Yu. L. Smorodin, JETP **36**, 1159 (1959), Soviet Phys. JETP **9**, 823 (1959); Bogachev, Bunyatov, Merekov, and Sidorov, DAN SSSR **121**, 617 (1958), Soviet Phys. Doklady **3**, 785 (1959).

[2] Belyakov, Wang, Glagolev, Dalkhazhava, Lebedev, Mel'nikov, Nikitin, Petrzilka, Sidorov, Suk, and Tolstov, JETP **39**, 937 (1960), Soviet Phys. JETP **12**, 650 (1961).

[3] Birger, Wang, Wang, Ting, Katyshev, Kladnitskaya, Kopylova, Lyubimov, Nguyen, Nikitin, Podgoretskiĭ, Smorodin, Solov'ev, and Trka, JETP **41**, 1461 (1961), Soviet Phys. JETP **14**, 1043 (1962).

[4] V. S. Barashenkov, Joint Institute for Nuclear Research, Preprint R-540, 1960.

[5] Botvin, Takibaev, Chasnikov, Pavlova, and Boos, JETP **41**, 993 (1961), Soviet Phys. JETP **14**, 705 (1962).

[6] Visky, Podgoretskiĭ, and Gramenitskiĭ, Joint Institute for Nuclear Research, Preprint R-636, 1960.

[7] Grote, Klabuhn, Krecher, Kundt, Lanius, and Meier, Nuclear Phys. (in press).

[8] Vinitskiĭ, Golyak, Pavlova, Takibaev, and Rus'kin, Proc. Nucl. Phys. Inst., Acad. Sci. Kazakh S.S.R. (in press).

[9] Boos, Botvin, Pavlova, Takibaev, and Chasnikov, JETP **42**, 3 (1962), Soviet Phys. JETP **15**, 1 (1962).

[10] I. M. Dremin, JETP **39**, 130 (1960), Soviet Phys. JETP **12**, 94 (1961); Gramenitskiĭ, Dremin, and Chernavskiĭ, JETP **41**, 856 (1961), Soviet Phys. JETP **14**, 613 (1962).

[11] V. I. Rus'kin, Proc. Nucl. Phys. Inst., Acad. Sci., Kazakh S.S.R. (in press).

[12] V. I. Rus'kin, Vestnik Acad. Sci. Kazakh S.S.R. **4**, 80 (1961).

Translated by E. Marquit
73